Cell Reports

Challenges in Establishing Pure Lung Cancer Organoids Limit Their Utility for Personalized Medicine

Graphical Abstract

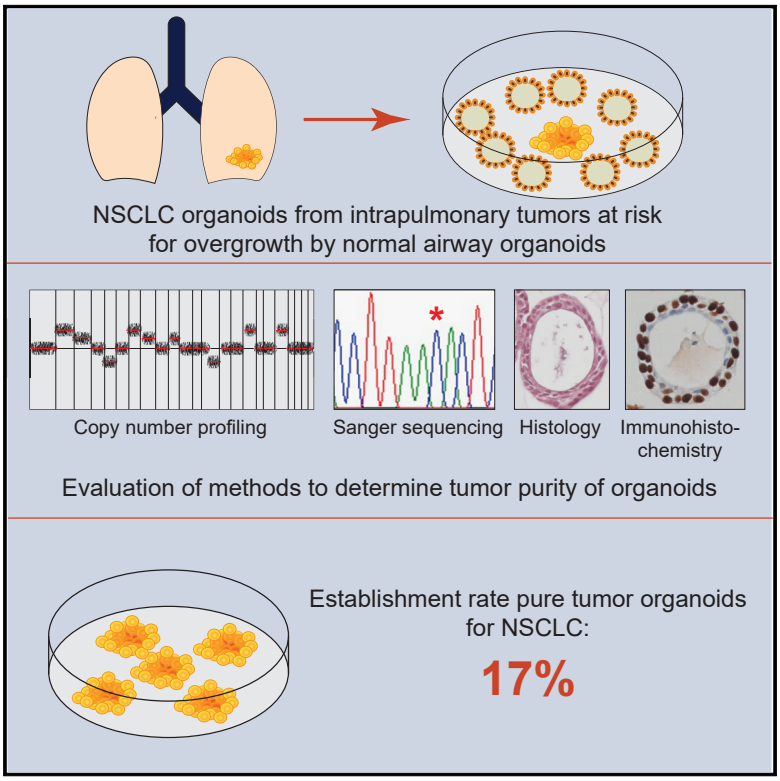

Highlights

- Frequent overgrowth of lung cancer organoids by normal airway organoids
- Copy number profiling and IHC can be used to distinguish tumor and normal organoids
- Low establishment rate of pure lung cancer organoids limits their clinical utility

Authors

Krijn K. Dijkstra, Kim Monkhorst, Luuk J. Schipper, ..., Hans Clevers, Edwin Cuppen, Emile E. Voest

Correspondence

e.voest@nki.nl

In Brief

Using a combination of genetic analyses and immunohistochemistry, Dijkstra et al. find that the majority of organoids derived from intrapulmonary lung cancers are overgrown by normal airway organoids. This limits the overall establishment rate of pure lung cancer organoids to 17%, restricting their utility for personalized medicine.

Dijkstra et al., 2020, Cell Reports *31*, 107588
May 5, 2020 © 2020 The Author(s).
https://doi.org/10.1016/j.celrep.2020.107588

Cell Reports

CellPress
OPEN ACCESS

Report

Challenges in Establishing Pure Lung Cancer Organoids Limit Their Utility for Personalized Medicine

Krijn K. Dijkstra,[1,11] Kim Monkhorst,[2] Luuk J. Schipper,[1,11] Koen J. Hartemink,[3] Egbert F. Smit,[4] Sovann Kaing,[1,11] Rosa de Groot,[5,6,11] Monika C. Wolkers,[5,6,11] Hans Clevers,[7,8,11] Edwin Cuppen,[9,10,11] and Emile E. Voest[1,11,12,*]

[1]Department of Molecular Oncology and Immunology, the Netherlands Cancer Institute – Antoni van Leeuwenhoek Hospital, 1066 CX Amsterdam, the Netherlands
[2]Department of Pathology, the Netherlands Cancer Institute – Antoni van Leeuwenhoek Hospital, 1066 CX Amsterdam, the Netherlands
[3]Department of Surgery, the Netherlands Cancer Institute – Antoni van Leeuwenhoek Hospital, 1066 CX Amsterdam, the Netherlands
[4]Department of Thoracic Oncology, the Netherlands Cancer Institute – Antoni van Leeuwenhoek Hospital, 1066 CX Amsterdam, the Netherlands
[5]Department of Hematopoiesis, Sanquin Research, 1066 CX Amsterdam, the Netherlands
[6]Landsteiner Laboratory, Amsterdam University Medical Center, Location AMC, 1105 AZ Amsterdam, the Netherlands
[7]Hubrecht Institute, University Medical Center Utrecht, 3584 CT Utrecht, the Netherlands
[8]Princess Maxima Center for Pediatric Oncology, 3584 CS Utrecht, the Netherlands
[9]Centre for Molecular Medicine, University Medical Centre Utrecht, 3584 CG Utrecht, the Netherlands
[10]Hartwig Medical Foundation, 1098 XH Amsterdam, the Netherlands
[11]Oncode Institute, Utrecht, the Netherlands
[12]Lead Contact
*Correspondence: e.voest@nki.nl
https://doi.org/10.1016/j.celrep.2020.107588

SUMMARY

Clinical implementation of tumor organoids for personalized medicine requires that pure tumor organoids can be reliably established. Here, we present our experience with organoid cultures from >70 non-small cell lung cancer (NSCLC) samples. We systematically evaluate several methods to identify tumor purity of organoids established from intrapulmonary tumors. Eighty percent of organoids from intrapulmonary lesions have a normal copy number profile, suggesting overgrowth by normal airway organoids (AOs). This is further supported by the failure to detect mutations found in the original tumor in organoids. Histomorphology alone is insufficient to determine tumor purity, but when combined with p63 immunostaining, tumor and normal AOs can be distinguished. Taking into account overgrowth by normal AOs, the establishment rate of pure NSCLC organoids is 17%. Therefore, current methods are insufficient to establish pure NSCLC organoids from intrapulmonary lesions. We discourage their use unless steps are taken to prevent overgrowth by normal AOs.

INTRODUCTION

The discovery that tumor cells can be efficiently cultured as organoids (reviewed in Drost and Clevers, 2018; Weeber et al., 2017) has been welcomed with great enthusiasm and has inspired studies that evaluate the feasibility of tumor organoids as tools for personalized medicine. Indeed, gastroesophageal, colorectal (Vlachogiannis et al., 2018), and pancreatic (Tiriac et al., 2018) cancer organoids show similar chemosensitivity as the patient's tumor, and organoids can prospectively predict response to irinotecan-based chemotherapy for colorectal cancer (Ooft et al., 2019).

However, for their clinical implementation, it is essential that organoids can be reliably generated with a high success rate. An additional challenge when culturing cancer samples from primary tumors is potential overgrowth by normal epithelial cells. For example, prostate cancer organoids can only be reliably established from metastases because normal prostate epithelial cells overgrow primary prostate cancer cells (Drost et al., 2016; Gao et al., 2014). Challenges in efficiently establishing (pure) tumor organoids could have major implications for the translational potential of tumor organoids.

A tumor type for which organoid-guided clinical decision making could be of particular value is non-small cell lung cancer (NSCLC). The frequent occurrence of aberrations in targetable genes such as *EGFR* or *ALK* provides opportunities for targeted therapies. However, resistance inevitably develops, and optimal treatment after standard of care is often unclear. Drug sensitivity of patient-derived tumor organoids could potentially guide treatment selection.

Here we describe our experience with >70 lung (cancer) organoids derived from NSCLC patients. We report culture success

This is an open access article under the CC BY-NC-ND license (http://creativecommons.org/licenses/by-nc-nd/4.0/).

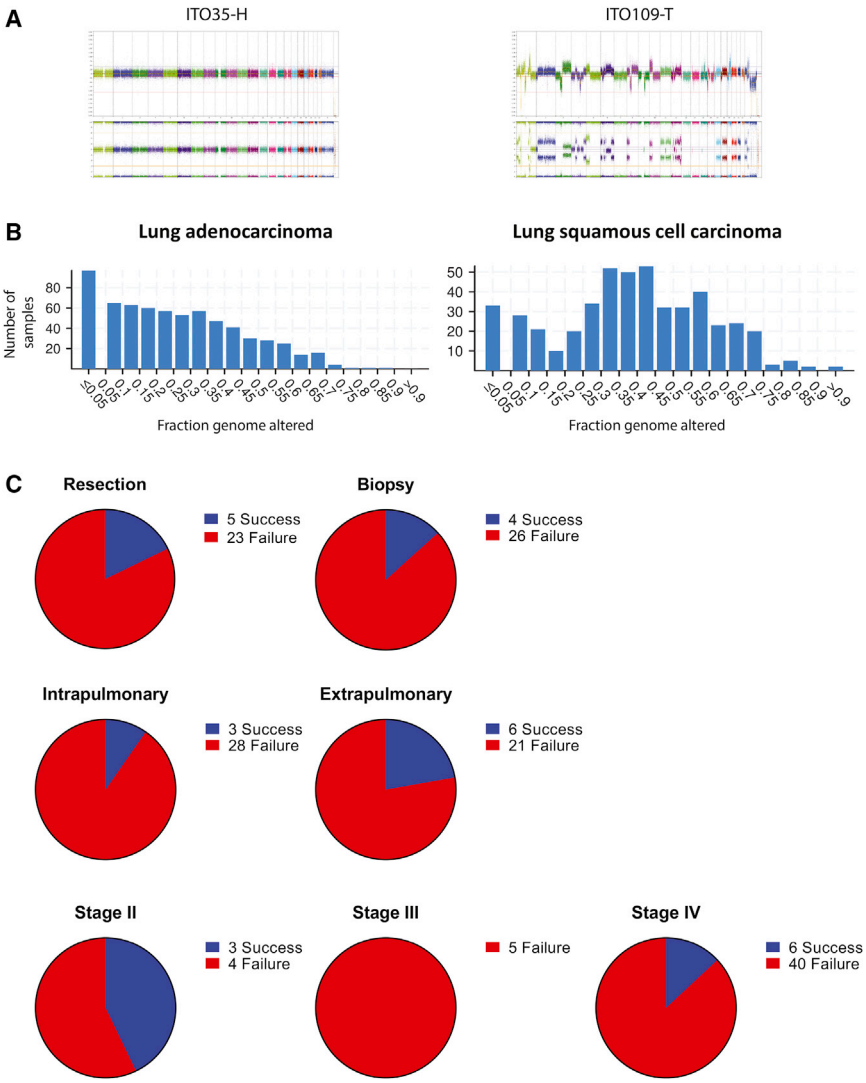

Figure 1. Copy Number Profiles and Culture Establishment Rates of Lung Cancer Organoids

(A) Examples of copy number profiles of normal airway organoids (left) or organoids derived from an extrapulmonary metastasis (right). Top part shows copy number centered on 2n chromosomes and expressed on a $\log_2$ scale. Bottom part indicates proportional expression of single-nucleotide polymorphisms (SNPs) used to determine copy number.

(B) Histogram of fraction of genome altered by copy number events of lung adenocarcinomas or squamous cell carcinomas. Results are based on data from Campbell et al., 2016 and derived from cbioportal (Cerami et al., 2012; Gao et al., 2013). Fraction of copy number altered represents the length of segments with copy number alteration value > 0.2 divided by the length of all segments.

(C) Success rate of tumor organoid establishment from different sources. Significance was determined using Fisher's exact test, including the Freeman-Halton extension for 2 × 3 tables, and no bias was found toward stage, location, or whether the sample was derived via a biopsy or a resection. See Figure S1 and Table S1.

rate and challenges to generate and identify pure tumor organoids. These results should inform the design of future studies that make use of NSCLC organoids.

RESULTS

Establishment of Normal Airway and NSCLC Organoids

We received NSCLC or macroscopically inconspicuous healthy lung tissue for organoid cultures, via surgical resections or core needle biopsies, of both intrapulmonary lesions and extrapulmonary metastases. We collected tissue of 46 adenocarcinomas, 4 squamous cell carcinomas (SCCs), 2 large cell neuroendocrine carcinomas, and 7 NSCLC samples that were not otherwise specified. Samples covered different tumor stages, with the majority being stage IV adenocarcinomas.

Overall, organoid establishment rate was 41% for tumor samples and 46% for normal samples. Mindful of potential overgrowth of cancer organoids by normal epithelial tissue (Drost et al., 2016), we systematically evaluated the utility of several approaches to determine tumor purity of organoid cultures, including copy number (CN) profiling, the detection of mutations in cancer genes, histomorphological features, and immunohistochemistry (IHC).

Determination of Tumor Purity by Genetic Analysis

We first generated CN profiles from organoids derived from intrapulmonary lung cancers. In addition, CN profiles were generated for normal airway organoids (AOs) and extrapulmonary cancer organoids. All 5 AOs showed normal CN profiles (Figure 1A; Figure S1A; Table 1), and all 5 extrapulmonary tumor organoids showed multiple gains and losses (Figure 1A; Figure S1B; Table 1). However, of 20 organoids derived from intrapulmonary tumors, as many as 16 (80%) showed normal CN profiles (Figure S1C; Table 1). We assessed the distribution of CN profiles in lung cancer on the basis of The Cancer Genome Atlas (TCGA) data (Campbell et al., 2016; Cerami et al., 2012; Gao et al., 2013). A subset of primary NSCLC samples in TCGA shows normal CN profiles, but these do not exceed 15% of adenocarcinomas or 7% of SCCs (Figure 1B). If these rates were extrapolated to our cohort of intrapulmonary tumors, only 3 organoids are expected to have normal CN profiles. This suggests that the majority (estimated at 65%) of organoids derived from intrapulmonary lesions are overgrown by healthy AOs.

Tumor organoids contain mutations in cancer genes found in the original tumor (Weeber et al., 2015; van de Wetering et al., 2015). We therefore systematically evaluated the presence of mutations in a small panel of cancer genes. A subset of

Table 1. Copy Number Profiles, Histomorphology, Immunohistochemistry, and Mutations of Organoids Derived from Healthy Lung Tissue and Extrapulmonary or Intrapulmonary NSCLC Tumors

Sample	Copy Number Profile	Morphology	TTF-1	p63	CK5/6	Mutation in Original Tumor	Mutation Detected in Organoids
Normal Airway Organoids							
Lung-1-H	normal	cystic	++	+/− (polarized)	N/A	N/A	N/A
ITO34-H (handpicked)	normal	cystic	++	+/− (polarized)	++	N/A	N/A
ITO35-H	normal	cystic	++	+/− (polarized)	++	N/A	N/A
ITO54-H	normal	cystic	++	+/− (polarized)	++	N/A	N/A
ITO62-H	N/A	cystic	++	+/− (polarized)	++	N/A	N/A
ITO83-H	normal	cystic/solid	++	+/− (polarized)	n/a	N/A	N/A
ITO151-H	N/A	cystic/solid	++	+/− (polarized)	n/a	N/A	N/A
ITO154-H	N/A	cystic	++	+/− (polarized)	n/a	N/A	N/A
Organoids from Extrapulmonary Tumors							
ITO42-T	abnormal	solid	++	−	−	N/A	N/A
ITO109-T	abnormal	solid	−	−	−	N/A	N/A
ITO120-T	abnormal	solid	+/− (heterogeneous)	+/− (non-polarized)	+/− (focal)	N/A	N/A
ITO127-T	abnormal	solid	++/− (heterogeneous)	−	−	KRAS c.34G>A	yes
ITO142-T	abnormal	N/A	N/A	N/A	N/A	N/A	N/A
Organoids from Intrapulmonary Tumors (Abnormal Copy Number Profile)							
ITO31-T1	abnormal	mostly cystic, some solid	N/A	N/A	N/A	N/A	N/A
ITO34-T, Nutlin selected	abnormal	solid	−	−	−	N/A	KRAS c.34G>T STK11 c.725G>T
ITO148-T A	abnormal	solid	N/A	N/A	−	N/A	N/A
ITO148-T B	abnormal	N/A	N/A	N/A	N/A	N/A	N/A
Organoids from Intrapulmonary Tumors (Normal Copy Number Profile)							
Lung-1-T	normal	cystic	N/A	N/A	N/A	N/A	N/A
ITO21-T1	normal	mostly solid, some cystic	++	+/− (polarized)	++/−	KRAS c.183A > T	no
ITO21-T2	n/a	mostly cystic, some solid	N/A	N/A	N/A	N/A	N/A
ITO22-T	normal	solid	++/−	++/−	++	KRAS c.35G > T	no
ITO24-T	normal	cystic	++	+/− (polarized)	N/A	N/A	N/A
ITO31-T2	normal	cystic	++	+/− (polarized)	N/A	N/A	N/A
ITO34-T (unselected)	normal	cystic	N/A	N/A	N/A	N/A	N/A
ITO41-T	normal	cystic	++	+/− (polarized)		EGFR c.2369C>T	no
ITO54-T	normal	cystic	++	+/− (polarized)	++/−	N/A	N/A
ITO62-T	normal	solid	+/−	+		FLT3 c.1948del	no

(*Continued on next page*)

Table 1. *Continued*

Sample	Copy Number Profile	Morphology	TTF-1	p63	CK5/6	Mutation in Original Tumor	Mutation Detected in Organoids
ITO74-T	normal	cystic	+/− (heterogeneous)	+/− (polarized)	+/−	KRAS c.182A>T	no
ITO83-T	normal	cystic	++	+/− (polarized)	N/A	KRAS c.34G>T	no
ITO97-T	normal	solid	++/−	+/− (inverted)	N/A	KRAS c.34G>T	no
ITO123-T	normal	cystic	n/a	n/a	N/A	KRAS c.35G>A	no
ITO128-T	normal	mostly solid, some cystic	+/−	+/− (polarized)	N/A	KRAS c.34G>T	no
ITO133-T	normal	cystic	++	+/− (polarized)	++	KRAS c.180_181delinsAA	no
ITO135-T	normal	cystic	++	+/− (polarized)	N/A	N/A	N/A

Mutations were detected using PCR followed by Sanger sequencing, except for ITO22-T/ITO34-T (whole-genome sequencing) and ITO41-T (whole-exome sequencing). Nomenclature is based on coding DNA reference sequence NM_004985.4 (KRAS), NM_005228.3 (*EGFR*), NM_004119.2 (*FLT3*), and NM000455.4 (*STK11*). Immunohistochemistry staining varies among negative (−), weakly positive (+), and strongly positive (++). Heterogeneous p63 staining within one organoid could either be non-polarized or polarized, with strong expression on the outer edge and loss of expression at the luminal side. Cystic organoids with a normal copy number profile grew out without selection for ITO34-T. After selection with the MDM2-inhibitor Nutlin-3a, solid tumor organoids with an abnormal copy number profile were generated. Hand-picking cystic organoids resulted in a pure culture of cystic organoids with normal copy number profile. See Table S1.

intrapulmonary tumors harbored mutations in cancer genes such as *EGFR*, *KRAS*, *FLT3*, and *STK11*. Of ten intrapulmonary tumors with mutations in these genes, in none of the organoids derived thereof the mutation could be detected (Table 1). This further supports the notion that a large fraction of organoids derived from intrapulmonary tumors are overgrown by normal AOs.

Determination of Tumor Purity by Histomorphology

Although the generation of CN profiles is relatively fast and affordable, simple morphological features may even be easier in classifying organoids as tumor or normal. We therefore prepared hematoxylin and eosin (H&E)-stained slides of lung (cancer) organoids. Normal AOs grew mostly as relatively well-organized cystic structures with an outer edge one or two cells thick, but for some cultures (ITO83-H, ITO151-H, and less prominently in Lung-1-H), more solid organoids were also present (Figure 2A; Figure S2A). This indicates that a solid morphology does not exclude the presence of normal AOs.

Most confirmed tumor organoids (because of extrapulmonary origin or abnormal CN profiles) grew as irregular solid structures, except for ITO31-T1, an early-stage cancer that showed more cystic/cribriform growth (Figure 2B; Figures S2B and S2C). Some organoids (ITO42-T) showed signs of tube formation, although their small size makes the interpretation challenging. These two cultures were difficult to distinguish from ITO83-H and ITO151-H on the basis of histomorphological criteria. Tumor organoids can therefore be both cystic or solid.

Organoids derived from intrapulmonary lesions that could not be classified as tumor organoids on the basis of CN profiles differed greatly in histomorphology (Figure 2C; Figure S3). Organoids such as Lung-1-T, ITO41-T, and ITO54-T grew as cystic, thin-layered organized structures that resembled normal AOs. In contrast, organoids such as ITO22-T and ITO62-T grew as solid masses. The majority of organoids did not grow as solid masses, but also not as symmetrical cystic structures, and showed intercellular variation in cell size, nuclear shape, and polarity (e.g., ITO24-T, ITO83-T, ITO74-T). This group is particularly challenging to classify as tumor or normal, as they share features of both normal AOs and organoids derived from extrapulmonary metastases.

Determination of Tumor Purity by IHC

Because tumor and normal AOs could not be distinguished on the basis of histomorphological features alone, we evaluated whether IHC could aid in the development of a classifier. We stained organoids for thyroid transcription factor 1 (TTF-1), a marker normally expressed in type II pneumocytes and club cells in the lung, and tumor protein 63 (p63), expressed in basal cells of respiratory epithelium. NSCLC adenocarcinomas are generally distinguished from SCCs on the basis of the expression of TTF-1 in the former and p63 in the latter (but rarely both) (Kim et al., 2013).

Normal AOs showed strongly positive TTF-1 staining in virtually all cells (Figure 3A). Staining for p63, however, showed a polarized pattern in which the outer cellular ring was positive, and intraluminal cells were negative, similar to expression in normal lung (Wang et al., 2002). In contrast, none of the confirmed tumor organoids (because of extrapulmonary origin or abnormal CN profile) that were evaluated showed this pattern. So tumor organoids invariably showed loss of this characteristic, polarized p63 staining pattern. p63 expression was either completely negative or heterogeneous and disorganized (ITO120-T) (Figure 3B).

Almost all organoids derived from intrapulmonary tumors that showed normal CN profiles showed the typical p63 staining pattern seen in normal AOs (Figure 3C). Two exceptions were ITO22-T and ITO62-T, which grew as solid masses instead of spheres. Here, p63 expression was also seen more strongly at the outer edge and lost in the center. This is reminiscent of

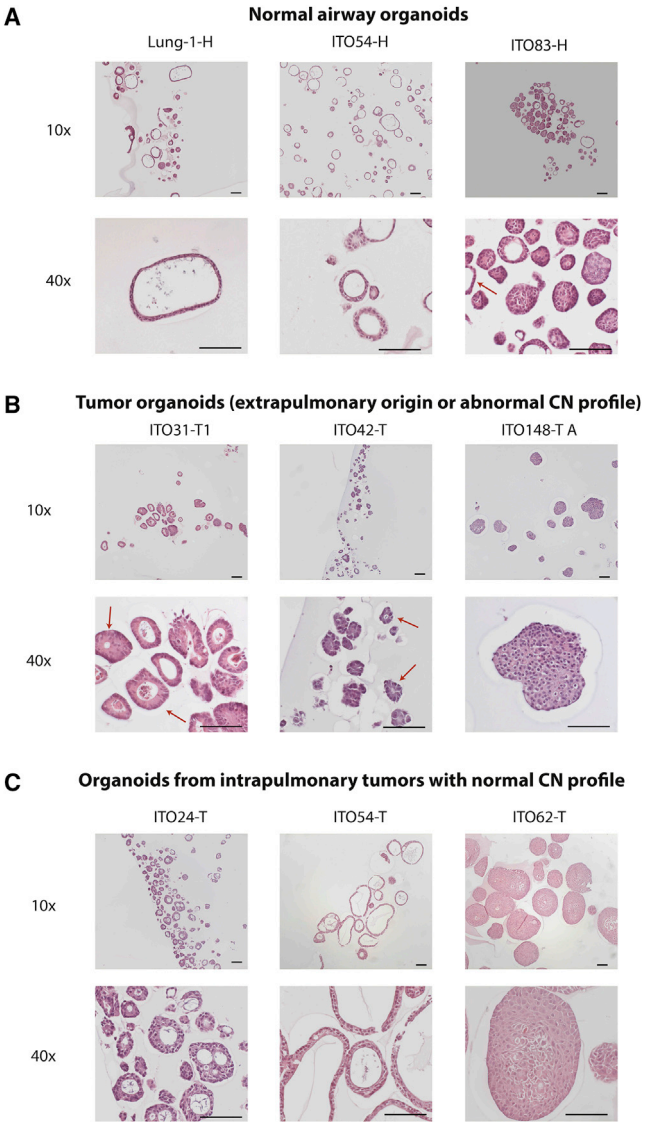

Figure 2. Examples of Hematoxylin and Eosin-Stained Slides of Lung (Cancer) Organoids

Pictures taken at 10× or 40× magnification. Scale bar, 100 μm. Examples of tube formation are indicated by red arrows.

(A) Normal airway organoids. Note the predominantly cystic morphology with slim cellular contours but also more infrequent presence of solid organoids.

(B) Tumor organoids. Note the predominantly solid irregular morphology. ITO31-T1 shows also more cystic organoids. Signs of tube formation are also seen in ITO42-T.

(C) Organoids derived from intrapulmonary tumors. Note the wide variety of morphologies, varying from thin and cystic (ITO54-T), through increasing stages of disorganization (ITO24-T), to solid spheres (ITO62-T).

See Figures S2 and S3.

loss of p63 expression as squamous epithelial cells mature (Wang et al., 2002). Indeed, these organoids appeared histomorphologically as squamous epithelial cells. Of note, ITO62-T organoids were derived from an SCC, but ITO22-T organoids were derived from an adenocarcinoma. Together with the normal CN profile and absence of the *KRAS* (ITO22-T) or *STK11* (ITO62-T) mutations that were present in the original tumor, this is highly suggestive of outgrowth of non-malignant cells that show metaplasia in culture.

These data suggest that a classifier could be conceived on the basis of the combination of histomorphology and the pattern of p63 expression (Table 1). Spherical organoids that show polarized p63 expression can be considered normal AOs. Organoids that show more solid morphology can also be considered normal AOs if polarized p63 expression is present (as for ITO22-T and ITO62-T).

To extend our IHC panel, we also stained organoids for cytokeratin 5/6 (CK5/6) which is normally expressed in basal airway cells. Expression of CK5/6 was observed in normal AOs derived from normal lung tissue but also in organoids derived from intrapulmonary lesions that were overgrown by normal AOs (Figure S4A; Table 1). In contrast, confirmed tumor organoids were largely negative for CK5/6 (Figure S4B; Table 1). This suggests that staining for CK5/6 together with p63 can provide additional certainty in differentiating between tumor and normal AOs. This differential staining pattern is also observed in patient tissue (Figure S4C): normal bronchial airway epithelium is positive for TTF-1, p63 (polarized), and CK5/6. In contrast, tumors can be positive for p63, but polarization is lost. Tumors usually do not express CK5/6, although it can be seen in basaloid SCC such as ITO31-T1.

Selection for Tumor Cells

Methods to select for tumor cells at an early stage could improve the quality of the culture of intrapulmonary NSCLC organoids (Wallaschek et al., 2019). For example, *TP53*-mutated organoids could be selected for by the addition of the MDM2 inhibitor Nutlin-3a (Sachs et al., 2019). As an example, one of our organoids derived from an intrapulmonary tumor (ITO34-T) was overgrown by normal AOs without selection. Upon Nutlin selection, however, we established a pure culture consisting of solid tumor organoids (Dijkstra et al., 2018). In this case, normal AOs showed a different morphology and could be manually picked out from the culture on the basis of their cystic shape. Normal AOs and tumor organoids from this patient showed distinct CN profiles, histomorphology, and p63/TTF-1 staining patterns (Figure 4).

This strategy may not be successful for all samples, first because *TP53* mutations are present in many but not all NSCLC cases (Campbell et al., 2016) and second because these mutations may also be present in normal lung cells because of field cancerization (Gao et al., 2009; Curtius et al., 2018). Recently, the establishment of pure lung cancer organoids using a minimal medium, not permissive to growth of normal AOs, has been described (Kim et al., 2019). Whether Nutlin-based or other selection strategies (Kim et al., 2019) result in higher tumor purity without compromising organoid establishment rate needs to be established in larger cohorts.

In summary, the success rate of establishing tumor organoids is largely affected by overgrowth by normal AOs. Organoids were established from tumor specimens in 24 of 58 cases (41%), but 14 of these appear to be normal AOs. This resulted in an overall success rate of only 17%. There was no significant difference in establishment rate depending on stage, tumor location, or whether the material was obtained via a biopsy or surgical resection (Figure 1C; Table S1).

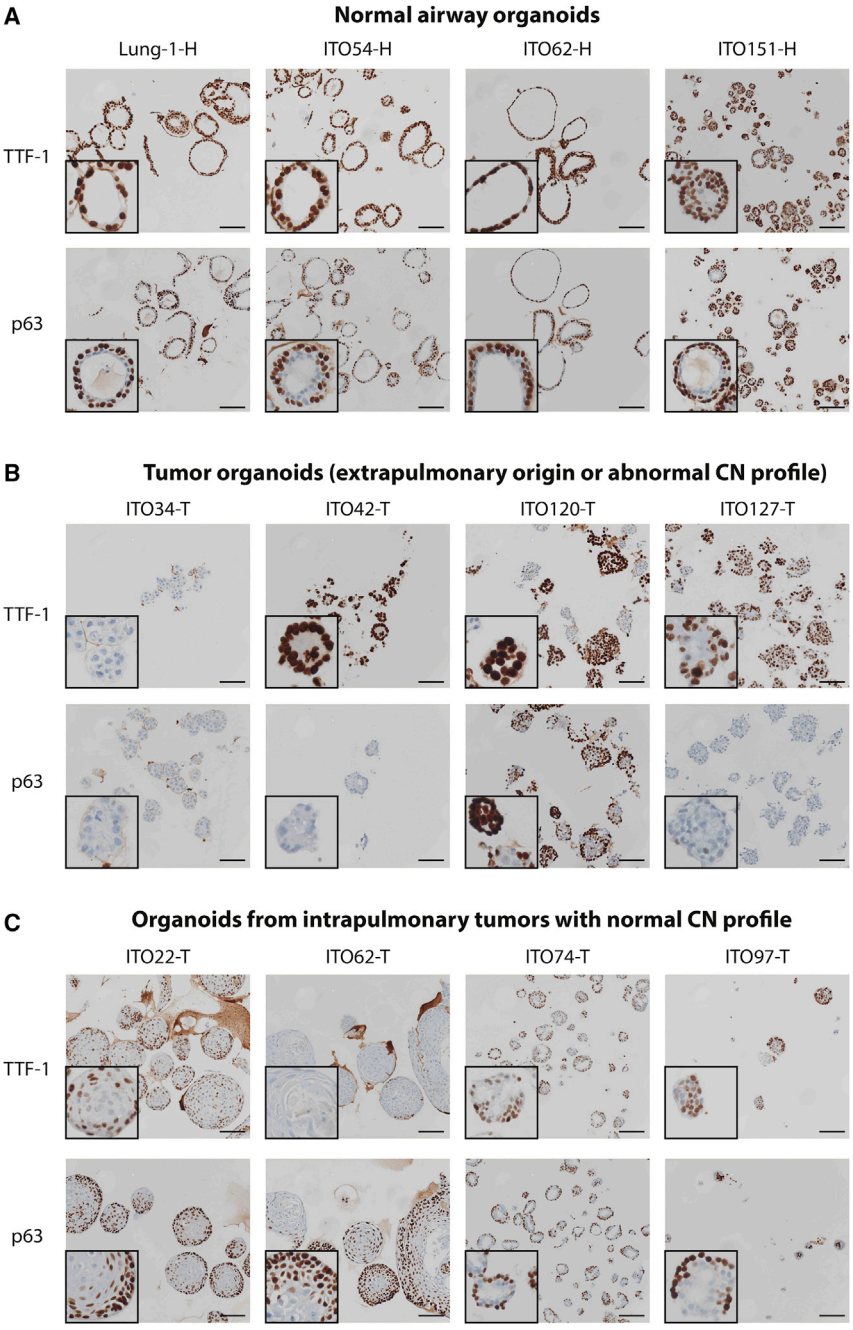

Figure 3. Examples of TTF-1 and p63 Staining of Lung (Cancer) Organoids

Pictures taken at 20× magnification. Scale bar, 100 μm. Insets represent images magnified an additional 3× (60×).

(A) Normal airway organoids. Note uniform TTF-1 positivity and polarized p63 expression.

(B) Tumor organoids. Note loss of polarized p63 expression.

(C) Organoids with a normal CN profile, derived from intrapulmonary tumors. Note solid balls with polarized p63 expression (ITO22-T and ITO62-T), polarized p63 expression mirroring normal AOs (ITO74-T), and inversion of p63 polarization (ITO97-T).

See Figure S4.

DISCUSSION

Taken together, establishment of NSCLC organoids faces several challenges. The vast majority (80%) of organoids derived from intrapulmonary tumors were overgrown by normal AOs, as shown by a normal CN profile and the absence of mutations present in the original tumor. Overgrowth by normal AOs is not a concern for extrapulmonary metastases, but the success rate of only 21% for biopsies of metastases significantly limits clinical implementation.

Reliable classification of lung organoid cultures as tumor or normal is therefore essential. CN profiling can unambiguously identify the majority of samples as either tumor or normal. Importantly, hybrid cultures of normal and tumor organoids likely exist in the early stages of culturing, which complicates the interpretation of drug screens. Tumor purity could be estimated by CN profiling on the basis of the minor allele frequency. Note that in mixed cultures, a small subpopulation of normal AOs may eventually dominate the culture. Therefore, repeated evaluation of tumor purity will be important for mixed tumor/normal cultures. Whole-genome or panel sequencing may complement CN profiling to classify organoids derived from tumors with relatively normal CN profiles.

Classification based on histomorphology is more ambiguous than CN-based classification. Growth patterns form a spectrum ranging from well-organized, monolayered, cystic organoids to highly disorganized solid masses. Tumor organoids and normal AOs can appear both as cystic or solid organoids. Therefore, histology alone will unlikely be sufficient to reliably classify all samples.

When combined with p63 immunostaining, normal AOs and tumor organoids can be more easily distinguished. There appear to be three different phenotypes. First, most normal organoids are cystic with polarized p63 expression. Second, tumor organoids can be either cystic or solid but show loss of this characteristic p63 expression pattern. Third, a small subset of organoids grow as organized, solid masses, which also show polarized p63 expression to some extent (ITO22-T and ITO62-T). Because they show normal CN profiles and lack mutations found in the original tumor, these organoids are considered non-malignant and most likely represent metaplastic squamous epithelial cells. Whether such a classifier can be reliably used to classify organoids as tumor or normal should be validated in an independent cohort.

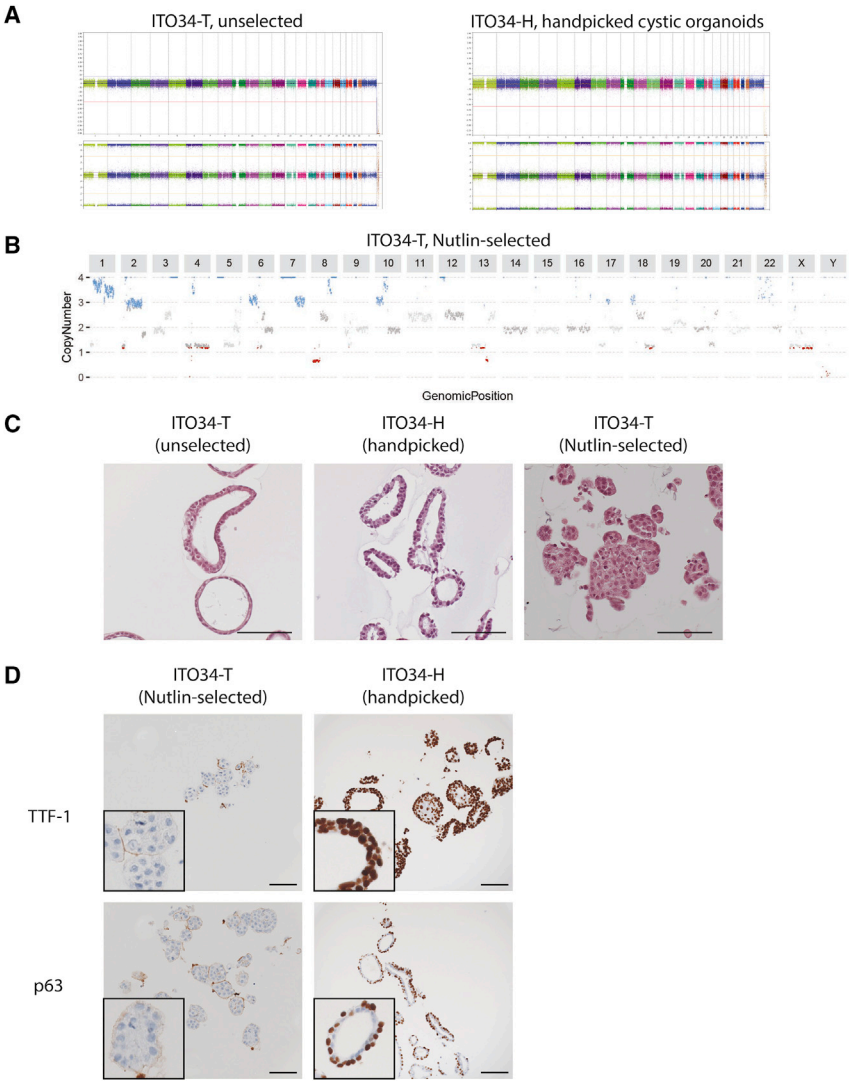

Figure 4. Selection of Tumor Organoids Using Nutlin

Organoids derived from ITO34-T were overgrown by normal AOs without applying selection. Applying the MDM-2 inhibitor Nutlin at an early stage of culture resulted in selection of pure tumor organoids. From mixed cultures, organoids with cystic morphology were handpicked and cultured separately as matched normal AOs.

(A) Copy number profiles of unselected or handpicked normal airway organoids. Top part shows copy number centered on 2n chromosomes and expressed on a $\log_2$ scale. Bottom part indicates proportional expression of single-nucleotide polymorphisms (SNPs) used to determine copy number.

(B) CN profile of Nutlin-selected tumor organoids. Whole-genome sequencing was used to determine copy number profile, expressed on a linear scale with number of chromosomes on the y axis.

(C) Hematoxylin and eosin-stained slides of unselected, handpicked normal AOs or tumor organoids from ITO34. Pictures taken at 40× magnification. Scale bar, 100 μm. Note the cystic morphology for normal AOs and the solid, irregular shape for selected tumor organoids.

(D) TTF-1 and p63 staining of ITO34 organoids. Pictures taken at 20× magnification. Scale bar, 100 μm. Insets represent images magnified an additional 3× (60×). Note uniform TTF-1 positivity and polarized p63 expression in handpicked normal AOs but loss of expression in Nutlin-selected tumor organoids.

Earlier studies have also commented on the challenge of obtaining pure tumor organoids from intrapulmonary lesions, and reported similar establishment rates for metastatic NSCLC (28%) (Sachs et al., 2019). This is still a large departure from the establishment rate of primary NSCLC cell lines (typically less than 5%) (Zheng et al., 2011; Sugaya et al., 2002). Therefore, although their establishment rate is too low for clinical implementation, NSCLC organoids do represent a valuable research tool. In particular, the ability to propagate and manipulate tumor cells derived from patients with different tumor characteristics makes it a versatile model. Alternative models such as tumor explantation systems (Padhye et al., 2019; Jenkins et al., 2018) generally do not allow expansion and extensive manipulation of tumor cells but are valuable to study tumors in their micro-environment.

We make four recommendations for the field to move forward. First, the establishment rate of tumor organoids should be increased. For some samples, tumor organoids may never have grown in the first place, and the only organoids that ever grew were normal AOs. Purging normal AOs will not be useful in those cases. Improving outgrowth of tumor organoids may be achieved in part by increasing the amount of starting material, for example by taking multiple biopsies. In addition, an understanding of biases in tumor outgrowth may help formulate culture media that are more permissive (Fujii et al., 2016). When sufficient material is available, compound screens may be an unbiased approach to optimize culture medium. Second, NSCLC organoids derived from intrapulmonary lesions should be routinely evaluated for tumor purity, using genetic methods or histomorphology combined with p63 and CK5/6 staining. *In vivo* tests of tumorigenicity can be considered if additional certainty is required. Third, the efficacy of selection strategies to purge normal AOs should be evaluated in large cohorts. In addition to selection based on culture media formulation, tumor purity may be increased by early separation of organoids with different morphologies (Wallaschek et al., 2019). Fourth, the feasibility of translational or clinical research projects that involve NSCLC organoid culture should be carefully evaluated given the low establishment rate of pure tumor organoids.

In conclusion, the potential use of NSCLC organoids for precision medicine is limited by low establishment rate and frequent overgrowth by normal AOs. We recommend restricting NSCLC organoid cultures to extrapulmonary lesions and discourage the use of intrapulmonary tumors unless rigorous methods are taken to prevent overgrowth by normal AOs.

STAR★METHODS

Detailed methods are provided in the online version of this paper and include the following:

- KEY RESOURCES TABLE
- RESOURCE AVAILABILITY
  - Lead contact
  - Materials availability
  - Data and code availability
- EXPERIMENTAL MODEL AND SUBJECT DETAILS
  - Patient tissue
  - Organoid establishment and culture
- METHOD DETAILS
  - Immunohistochemistry
  - Nutlin selection
  - DNA sequencing
  - PCR and Sanger sequencing
- QUANTIFICATION AND STATISTICAL ANALYSIS

SUPPLEMENTAL INFORMATION

Supplemental Information can be found online at https://doi.org/10.1016/j.celrep.2020.107588.

ACKNOWLEDGMENTS

We acknowledge Judith Westra, Sandra Visser, Louisa Hoes, Daphne van der Velden, Fleur Weeber, Xander Veenhof, and Houke Klomp for help with acquisition of patient tissue. We acknowledge the NKI-AVL Core Facility Molecular Pathology & Biobank (CFMPB) for supplying NKI-AVL Biobank material and lab support. Ron Kerkhoven, Marja Nieuwland, Roel Kluin, Charlaine Steenis, and Wim Brugman generated CN data for ITO41-T. We thank Chiara Cattaneo for support in organoid culture. This work was supported by the Dutch Cancer Society (HUBR 2014-7006) and the NWO Gravitation Program (NWO; 2012-2022) (to E.E.V.).

AUTHOR CONTRIBUTIONS

Conceptualization, K.K.D., E.F.S., E.C., H.C., and E.E.V.; Methodology, K.K.D., K.M., S.K., and E.C.; Investigation, K.K.D. and K.M.; Resources, L.J.S., K.J.H., E.F.S., S.K., R.G., and M.C.W.; Writing – Original Draft, K.K.D.; Writing – Review and Editing, K.M., L.J.S., K.J.H., E.F.S., M.C.W., E.C., and E.E.V.; Supervision, E.E.V.; Funding Acquisition, E.F.S., E.C., H.C., and E.E.V.

DECLARATION OF INTERESTS

H.C. declares the following management/advisory relationships: distinguished visiting professor, University of Hong Kong; member of the Scientific Advisory Board of Surrozen, San Francisco, California, USA; member of the Scientific Advisory Board of Kallyope, New York, USA; member of the Scientific Advisory Board of Merus, Utrecht, the Netherlands; scientific adviser to Life Science Partners, Amsterdam, the Netherlands; non-executive board member of Roche Holding Ltd., Basel, Switzerland.

Received: November 1, 2019
Revised: February 11, 2020
Accepted: April 8, 2020
Published: May 5, 2020

REFERENCES

Boeva, V., Popova, T., Bleakley, K., Chiche, P., Cappo, J., Schleiermacher, G., Janoueix-Lerosey, I., Delattre, O., and Barillot, E. (2012). Control-FREEC: a tool for assessing copy number and allelic content using next-generation sequencing data. Bioinformatics *28*, 423–425.

Campbell, J.D., Alexandrov, A., Kim, J., Wala, J., Berger, A.H., Pedamallu, C.S., Shukla, S.A., Guo, G., Brooks, A.N., Murray, B.A., et al.; Cancer Genome Atlas Research Network (2016). Distinct patterns of somatic genome alterations in lung adenocarcinomas and squamous cell carcinomas. Nat. Genet. *48*, 607–616.

Cerami, E., Gao, J., Dogrusoz, U., Gross, B.E., Sumer, S.O., Aksoy, B.A., Jacobsen, A., Byrne, C.J., Heuer, M.L., Larsson, E., et al. (2012). The cBio cancer genomics portal: an open platform for exploring multidimensional cancer genomics data. Cancer Discov. *2*, 401–404.

Curtius, K., Wright, N.A., and Graham, T.A. (2018). An evolutionary perspective on field cancerization. Nat. Rev. Cancer *18*, 19–32.

Dijkstra, K.K., Cattaneo, C.M., Weeber, F., Chalabi, M., van de Haar, J., Fanchi, L.F., Slagter, M., van der Velden, D.L., Kaing, S., Kelderman, S., et al. (2018). Generation of tumor-reactive T Cells by co-culture of peripheral blood lymphocytes and tumor organoids. Cell *174*, 1586–1598.e12.

Drost, J., and Clevers, H. (2018). Organoids in cancer research. Nat. Rev. Cancer *18*, 407–418.

Drost, J., Karthaus, W.R., Gao, D., Driehuis, E., Sawyers, C.L., Chen, Y., and Clevers, H. (2016). Organoid culture systems for prostate epithelial and cancer tissue. Nat. Protoc. *11*, 347–358.

ENCODE Project Consortium (2012). An integrated encyclopedia of DNA elements in the human genome. Nature *489*, 57–74.

Fujii, M., Shimokawa, M., Date, S., Takano, A., Matano, M., Nanki, K., Ohta, Y., Toshimitsu, K., Nakazato, Y., Kawasaki, K., et al. (2016). A colorectal tumor organoid library demonstrates progressive loss of niche factor requirements during tumorigenesis. Cell Stem Cell *18*, 827–838.

Gao, W., Mady, H.H., Melhem, M.F., and Keohavong, P. (2009). Analysis of p53 mutations in histologically normal lung tissues and lung tumors from non-small cell lung cancer patients. Mol. Carcinog. *48*, 633–641.

Gao, J., Aksoy, B.A., Dogrusoz, U., Dresdner, G., Gross, B., Sumer, S.O., Sun, Y., Jacobsen, A., Sinha, R., Larsson, E., et al. (2013). Integrative analysis of complex cancer genomics and clinical profiles using the cBioPortal. Sci. Signal. *6*, pl1.

Gao, D., Vela, I., Sboner, A., Iaquinta, P.J., Karthaus, W.R., Gopalan, A., Dowling, C., Wanjala, J.N., Undvall, E.A., Arora, V.K., et al. (2014). Organoid cultures derived from patients with advanced prostate cancer. Cell *159*, 176–187.

Jenkins, R.W., Aref, A.R., Lizotte, P.H., Ivanova, E., Stinson, S., Zhou, C.W., Bowden, M., Deng, J., Liu, H., Miao, D., et al. (2018). Ex vivo profiling of PD-1 blockade using organotypic tumor spheroids. Cancer Discov. *8*, 196–215.

Kim, M.J., Shin, H.C., Shin, K.C., and Ro, J.Y. (2013). Best immunohistochemical panel in distinguishing adenocarcinoma from squamous cell carcinoma of lung: tissue microarray assay in resected lung cancer specimens. Ann. Diagn. Pathol. *17*, 85–90.

Kim, M., Mun, H., Sung, C.O., Cho, E.J., Jeon, H.J., Chun, S.M., Jung, D.J., Shin, T.H., Jeong, G.S., Kim, D.K., et al. (2019). Patient-derived lung cancer organoids as in vitro cancer models for therapeutic screening. Nat. Commun. *10*, 3991.

Li, H. (2013). Aligning sequence reads, clone sequences and assembly contigs with BWA-MEM. arXiv, arXiv:1303.3997. https://arxiv.org/abs/1303.3997.

Ooft, S.N., Weeber, F., Dijkstra, K.K., McLean, C.M., Kaing, S., van Werkhoven, E., Schipper, L., Hoes, L., Vis, D.J., van de Haar, J., et al. (2019). Patient-derived organoids can predict response to chemotherapy in metastatic colorectal cancer patients. Sci. Transl. Med. *11*, eaay2574.

Opatz, S., Polzer, H., Herold, T., Konstandin, N.P., Ksienzyk, B., Zellmeier, E., Vosberg, S., Graf, A., Krebs, S., Blum, H., et al. (2013). Exome sequencing identifies recurring FLT3 N676K mutations in core-binding factor leukemia. Blood *122*, 1761–1769.

Padhye, A., Ungewiss, C., Fradette, J.J., Rodriguez, B.L., Albritton, J.L., Miller, J.S., and Gibbons, D.L. (2019). A novel ex vivo tumor system identifies Src-mediated invasion and metastasis in mesenchymal tumor cells in non-small cell lung cancer. Sci. Rep. *9*, 4819.

Priestley, P., Baber, J., Lolkema, M.P., Steeghs, N., de Bruijn, E., Shale, C., Duyvesteyn, K., Haidari, S., van Hoeck, A., Onstenk, W., et al. (2019). Pan-cancer whole-genome analyses of metastatic solid tumours. Nature *575*, 210–216.

Sachs, N., Papaspyropoulos, A., Zomer-van Ommen, D.D., Heo, I., Böttinger, L., Klay, D., Weeber, F., Huelsz-Prince, G., Iakobachvili, N., Amatngalim, G.D., et al. (2019). Long-term expanding human airway organoids for disease modeling. EMBO J. *38*, e100300.

Schneider, C.A., Rasband, W.S., and Eliceiri, K.W. (2012). NIH Image to ImageJ: 25 years of image analysis. Nat. Methods *9*, 671–675.

Shalaby, A.A., Presneau, N., Idowu, B.D., Thompson, L., Briggs, T.R., Tirabosco, R., Diss, T.C., and Flanagan, A.M. (2009). Analysis of the fibroblastic growth factor receptor-RAS/RAF/MEK/ERK-ETS2/brachyury signalling pathway in chordomas. Mod. Pathol. *22*, 996–1005.

Sugaya, M., Takenoyama, M., Osaki, T., Yasuda, M., Nagashima, A., Sugio, K., and Yasumoto, K. (2002). Establishment of 15 cancer cell lines from patients with lung cancer and the potential tools for immunotherapy. Chest *122*, 282–288.

Tiriac, H., Belleau, P., Engle, D.D., Plenker, D., Deschênes, A., Somerville, T.D.D., Froeling, F.E.M., Burkhart, R.A., Denroche, R.E., Jang, G.H., et al. (2018). Organoid profiling identifies common responders to chemotherapy in pancreatic cancer. Cancer Discov. *8*, 1112–1129.

van de Wetering, M., Francies, H.E., Francis, J.M., Bounova, G., Iorio, F., Pronk, A., van Houdt, W., van Gorp, J., Taylor-Weiner, A., Kester, L., et al. (2015). Prospective derivation of a living organoid biobank of colorectal cancer patients. Cell *161*, 933–945.

Vlachogiannis, G., Hedayat, S., Vatsiou, A., Jamin, Y., Fernández-Mateos, J., Khan, K., Lampis, A., Eason, K., Huntingford, I., Burke, R., et al. (2018). Patient-derived organoids model treatment response of metastatic gastrointestinal cancers. Science *359*, 920–926.

Wallaschek, N., Niklas, C., Pompaiah, M., Wiegering, A., Germer, C.T., Kircher, S., Brändlein, S., Maurus, K., Rosenwald, A., Yan, H.H.N., et al. (2019). Establishing pure cancer organoid cultures: identification, selection and verification of cancer phenotypes and genotypes. J. Mol. Biol. *431*, 2884–2893.

Wang, B.Y., Gil, J., Kaufman, D., Gan, L., Kohtz, D.S., and Burstein, D.E. (2002). P63 in pulmonary epithelium, pulmonary squamous neoplasms, and other pulmonary tumors. Hum. Pathol. *33*, 921–926.

Weeber, F., van de Wetering, M., Hoogstraat, M., Dijkstra, K.K., Krijgsman, O., Kuilman, T., Gadellaa-van Hooijdonk, C.G., van der Velden, D.L., Peeper, D.S., Cuppen, E.P., et al. (2015). Preserved genetic diversity in organoids cultured from biopsies of human colorectal cancer metastases. Proc. Natl. Acad. Sci. USA *112*, 13308–13311.

Weeber, F., Ooft, S.N., Dijkstra, K.K., and Voest, E.E. (2017). Tumor organoids as a pre-clinical cancer model for drug discovery. Cell Chem. Biol. *24*, 1092–1100.

Young, L., Sung, J., Stacey, G., and Masters, J.R. (2010). Detection of Mycoplasma in cell cultures. Nat. Protoc. *5*, 929–934.

Zheng, C., Sun, Y.H., Ye, X.L., Chen, H.Q., and Ji, H.B. (2011). Establishment and characterization of primary lung cancer cell lines from Chinese population. Acta Pharmacol. Sin. *32*, 385–392.

STAR★METHODS

KEY RESOURCES TABLE

REAGENT or RESOURCE	SOURCE	IDENTIFIER
Antibodies		
Mouse anti-human p63	ImmunoLogic	4A4;Cat#VWRKILM8651C1
Mouse anti-human TTF-1	Monosan	SPT24;Cat#MONX10584
Mouse anti-human Ker5/6	Roche	D5/16B4;790-4554
Biological Samples		
Patient tumor and normal lung tissue	the Netherlands Cancer Institute	study NL48824.031.14
Patient blood	the Netherlands Cancer Institute	study NL48824.031.14
Chemicals, Peptides, and Recombinant Proteins		
B27 supplement	GIBCO	Cat#17504-044
N-Acetylcysteine	Sigma-Aldrich	Cat#A9165-5G
Nicotinamide	Sigma-Aldrich	Cat#N0636
A83-01	Tocris	Cat#2939
SB202190	Cayman Chemicals	Cat#10010399
Y-27632	Sigma-Aldrich	Cat#Y-0503
Human recombinant FGF-7	Peprotech	Cat#100-19
Human recombinant FGF-10	Peprotech	Cat#100-26
Geltrex LDEV-free reduced growth factor basement membrane	GIBCO	Cat#A1413202
Collagenase type II	Sigma-Aldrich	Cat#C6885
Advanced DMEM-F12	GIBCO	Cat#12634-028
Penicillin/streptomycin	GIBCO	Cat#15070063
Ultraglutamine type I	Lonza	Cat#BE17-605E
HEPES	GIBCO	Cat#15630-056
TrypLE Express	GIBCO	Cat#12604-013
Recovery Cell Culture Freezing Medium	GIBCO	Cat#12648-010
Nutlin-3a	Cayman Chemicals	Cat#10004372
Dispase type II	Sigma-Aldrich	Cat#D4693
Primocin	Invivogen	Cat#ant-pm-1
Critical Commercial Assays		
DNeasy blood and tissue kit	QIAGEN	Cat#69504
MycoAlert Mycoplasma Detection Kit	Lonza	Cat#LT07-118
Deposited data		
Copy number / SNParray data of lung (cancer) organoids	This paper	Available on request from Netherlands Cancer Institute (IRB@nki.nl)
Whole exome sequencing data of lung (cancer) organoids	This paper	Available on request from Netherlands Cancer Institute (IRB@nki.nl)
Whole genome sequencing data of lung (cancer) organoids	This paper	Available on request from Netherlands Cancer Institute (IRB@nki.nl)
Experimental Models: Cell Lines		
L-Wnt3a cell line	Laboratory of Hans Clevers, Hubrecht Institute	L-Wnt3a
R-spondin producer cell line	Laboratory of Calvin Kuo, Stanford	293T-HA-Rspol-Fc
Noggin producer cell line	Laboratory of Hans Clevers, Hubrecht Institute	HEK293-mNoggin-Fc

(*Continued on next page*)

Continued

REAGENT or RESOURCE	SOURCE	IDENTIFIER
Software and Algorithms		
ImageJ version 1.50i	Schneider et al., 2012	https://imagej.nih.gov/ij/
GenomeStudio v2.0.4	Illumina	https://support.illumina.com/downloads/genomestudio-2-0.html
NxClinical	BioDiscovery	https://www.biodiscovery.com/products/NxClinical
Nexus Copy Number v10.0	BioDiscovery	https://www.biodiscovery.com/products/Nexus-Copy-Number
Zen v2.6	Zeiss	https://www.zeiss.com/microscopy/int/products/microscope-software/zen.html

RESOURCE AVAILABILITY

Lead contact

Requests for resources, reagents and further information should be addressed to the lead contact, Emile E. Voest (e.voest@nki.nl).

Materials availability

Material transfer agreements (MTA) are in place for producer lines for conditioned medium of Noggin (MTA with Hubrecht Institute) and R-spondin-1 (MTA with Calvin Kuo, Stanford). Requests for these resources should be directed to the relevant institutions.

Patient-derived organoids are available for sharing upon reasonable request as regulated by the signed informed consent and approved by the Medical Ethical Committee of the Netherlands Cancer Institute (study NL48824.031.14).

Data and code availability

Deposition of DNA sequencing data in publicly availably repositories is limited and regulated by the informed consent signed by patients participating in the study. Requests for sequencing and copy number data can be made by emailing the Institutional Review Board of the Netherlands Cancer Institute (IRB@nki.nl). Any other requests can be directed to the Lead author, Emile E. Voest (e.voest@nki.nl).

EXPERIMENTAL MODEL AND SUBJECT DETAILS

Patient tissue

Tissue was obtained from NSCLC patients undergoing surgery or receiving a 18G core needle tumor biopsy. Tumor tissue and macroscopically inconspicuous normal lung tissue (distant from the tumor site) were obtained for organoid culture. Tumor and normal tissue from the same patient share the same prefix (e.g., ITO54-T and ITO54-H, respectively). Written informed consent was obtained from all patients, and the study was approved by the Medical Ethical Committee of the Netherlands Cancer Institute – Antoni van Leeuwenhoek hospital (study NL48824.031.14). Tissue was stored in Ad-DF+++ (Advanced DMEM/F12 (GIBCO), with 1% Ultraglutamine I (GIBCO), 1% penicillin/streptomycin (GIBCO), 1% HEPES (GIBCO)) supplemented with 2% Primocin (Invivogen) at 4°C and processed for organoid culture within 24 hours. Organoids ITO22-T, ITO31-T1, ITO34-T, ITO41-T, ITO42-T, and ITO62-T have been described in Dijkstra et al., 2018 previously as (NSCLC-1 through NSCLC-6, respectively).

Organoid establishment and culture

Organoids were established and cultured as described in Sachs et al., 2019. Briefly, tumor or normal lung tissue was dissociated into small pieces using scalpels and digested for 30-60 minutes using 1.5 mg/mL collagenase II (Sigma-Aldrich), 2 mg/mL dispase type II (GIBCO), 10 μM Y-27632 (Sigma-Aldrich) and 1:500 Primocin in PBS. After digestion, cells were isolated by repeated resuspension and washed three times in PBS. Cells were plated in ice cold 10 mg/mL Geltrex (GIBCO) in 6-well culture plates. After letting Geltrex drops solidify for 15 minutes at 37°C, cells were overlaid with lung organoid medium, composed of Ad-DF+++ supplemented with 10% Noggin conditioned medium, 10% R-spondin-1 conditioned medium, 1x B27 supplement (GIBCO), 1.25 mM N-Acetylcystein (Sigma-Aldrich), 10 mM nicotinamide (Sigma-Aldrich), 25 ng/mL human recombinant FGF-7 (Peprotech), 100 ng/mL human recombinant FGF-10 (Peprotech), 500 nM A83-01 (Tocris), 1 μM SB202190 (Cayman Chemicals) and 5 μM Y-27632. Organoids were passaged every 1-2 weeks by incubating organoids for 5-10 minutes in TrypLE Express (GIBCO) at 37°C, followed by washing and replating in Geltrex. A culture was considered successful when expanded to $> 5*10^5$ organoids, upon which they were be cryopreserved in Recovery Cell Culture Freezing Medium (GIBCO). Samples were regularly tested for Mycoplasma contamination using a MycoAlert Mycoplasma Detection Kit (Lonza) or a PCR-based test (Young et al., 2010). Samples were authenticated by matching SNParray profiles of patient-derived blood and organoids, using a Taqman-based SNParray (Hartwig Medical Foundation, Amsterdam). Samples that could not be authenticated were considered failed cultures.

METHOD DETAILS

Immunohistochemistry

Organoids were isolated from Geltrex by resuspending in ice-cold PBS. Alternatively, organoids were incubated in 2 mg/mL dispase II for 15' at 37°C. Dispase was blocked by addition of 5 mM EDTA/PBS. Organoids were washed twice in PBS and fixed in 4% paraformaldehyde for 30 minutes or overnight at 4°C (protected from light). Organoids were then washed 2x in PBS, and the pellet was embedded in agarose. This was embedded in paraffin blocks, and 3 μm slides were sectioned. Routine hematoxylin and eosin (H&E) staining was performed. Immunohistochemistry was performed on a BenchMark Ultra autostainer (Ventana Medical Systems). Paraffin sections were heated at 75°C for 28 minutes and deparaffinized in the instrument with EZ prep solution (Ventana Medical Systems). Heat-induced antigen retrieval was carried out using Cell Conditioning 1 (CC1, Ventana Medical Systems) for 32 minutes (Ker 5/6), 40 minutes at 95°C (TTF-1), or 64 minutes at 95°C (P63). P63 was detected using clone 4A4 (1/800 dilution, 32 minutes at 36°C, ImmunoLogic), Ker 5/6 using clone D5/16B4 (Ready-To-Use, 32 minutes at 37°C, Roche Diagnostics) and TTF-1 using clone SPT24 (1/100 dilution, 32 minutes at 36°C, Monosan). Signal Amplification was performed for TTF-1 using the Optiview Amplification kit (Ventana Medical Systems). Bound antibody was detected using the OptiView DAB Detection Kit (Ventana Medical Systems). Slides were counterstained with Hematoxylin II and Bluing Reagent (Ventana Medical Systems).

Nutlin selection

ITO34-T organoids were cultured in NSCLC organoid medium with the addition of 5 μM Nutlin-3a (Cayman Chemicals) for four weeks. From unselected organoids, cystic organoids were handpicked with a P200 pipette tip using an inverted microscope. Organoids have been described previously (NSCLC-3 in Dijkstra et al. (2018).

DNA sequencing

Organoids were pelleted and DNA was isolated using a DNEasy blood and tissue kit (QIAGEN). Patient-matched blood was used for germline DNA. 50-200 ng DNA was used for SNParray (Illumina Cyto-SNP850k v1.2 according to suplier's protocols) to determine copy number profiles.

For ITO41-T, copy number profiles were determined using low-coverage whole genome sequencing (WGS) on an Illumina HiSeq2500 DNA analyzer (High Output Mode), and aligned to GRCh38 (Li, 2013). Read counts were binned (20 kb), rated against mappability, and log2 transformed. Correction for local GC effects was performed using a non-linear fit of mappabilities over 0.8 on autosomes. A linear fit was made of reference mappabilities after GC correction, and the slope was used to scale reference values. Bins with mappability < 0.2 or ENCODE blacklisted regions (ENCODE Project Consortium, 2012) were excluded.

For ITO34-T, copy number profiles were determined using WGS (TruSeq Nano LT library preparation and sequencing on Illumina HiSeqX to ~30x average depth according to standard supplier's protocols and settings). WGS data was analyzed using standardized tools (Priestley et al., 2019) and copy number profiles determined using Control-FREEC (Boeva et al., 2012).

PCR and Sanger sequencing

Primers for *KRAS* exon 2, *KRAS* exon 3 (Shalaby et al., 2009), and *FLT3* exon 16 (Opatz et al., 2013) were used to amplify exons with known oncogenic mutations in original tumors. PCR were run with 0.2 mM dNTPs, 1.5 mM MgCl2, 0.2 μM forward and reverse primer and 0.5 units Taq DNA polymerase (Biolabs). Sanger sequencing was performed by Macrogen (Amsterdam). *KRAS* exon 2 forward primer: 5′GATACACGTCTGCAGTCAACTG–3'; reverse primer: 5′-GGTCCTGCACAGTAATATGC-3′. *KRAS* exon 3 forward primer: 5′GATACACGTCTGCAGTCAACTG–3'; reverse primer: GGTCCTGCACAGTAATATGC-3′. *FLT3* exon 16 forward primer: 5′-TGCA GATTGACTCTGAGCTG-3′; reverse primer: 5′-CACTGTGACTGAGAAAAGACAAAG-3′.

QUANTIFICATION AND STATISTICAL ANALYSIS

SNParray data used for CN profiling was analyzed using GenomeStudio (Illumina) and visualized using NxClinical (BioDiscovery Inc). WGS data used for CN profiling was analyzed using Nexus Copy Number v10.0. Microphotographs were processed using Zen v2.6. Color balance for images in Figure S4 was optimized using ImageJ version 1.50i.

For Figure 1C, significance was determined using a Fisher's exact test, including the Freeman-Halton extension for 2x3 tables.